Conjugation of Poly-L-lysine to Bacterial Cytosine Deaminase Improves the Efficacy of Enzyme/Prodrug Cancer Therapy

Cong Li,* Flonne Wildes, Paul Winnard, Jr., Dmitri Artemov, Marie-France Penet, and Zaver M. Bhujwalla*

JHU ICMIC Program, The Russell H. Morgan Department of Radiology and Radiological Science, Johns Hopkins University School of Medicine, Baltimore, Maryland 21205

Received March 14, 2008

We previously observed that bacterial cytosine deaminase (bCD) conjugated with multimodal imaging reporter labeled poly-L-lysine (PLL) demonstrated high therapeutic efficacy in an enzyme/prodrug cancer therapeutic strategy. To understand the role of polycationic PLL in the cellular uptake of bCD−PLL conjugate, two control molecules, bCD−BF, without the PLL moiety, and bCD−AcPLL, with all positive charges in PLL neutralized, were prepared. bCD−PLL demonstrated about 50 times higher cellular uptake than that of control molecules in human breast MDA-MB-231 cancer cells. Internalized bCD−PLL demonstrated high enzymatic stability in cell cultures as indicated by significant cytotoxicity after addition of prodrug, whereas no obvious cytotoxicity was detected by control molecules. These data indicate that conjugated PLL not only provides a multivalent modification platform to facilitate the delivery of a high payload of imaging reporters or targeting moieties without compromising enzymatic activity but also enhances therapeutic efficacy by accelerating the intracellular uptake of prodrug-activating enzyme.

Introduction

The success of chemotherapy in the clinic is limited by insufficient drug concentrations in the tumor, lack of cancer cell specificity, systemic toxicity, and the development of drug resistance.[1,2] Enzyme/prodrug therapy is a promising solution to minimize systemic toxicity because the prodrug-activating enzyme is specifically delivered or expressed in cancer cells, followed by the systemic administration of a nontoxic prodrug.[3] The prodrug-activating enzyme localized within the tumor converts the prodrug to an active anticancer drug, achieving high concentration in the tumor, while normal tissue lacking the enzyme is spared of the toxic effect. Although limited success of enzyme/prodrug strategy has been achieved in preclinical studies,[4,5] several problems need to be resolved before its successful translation into the clinic. One of the most critical is to improve the less than optimal stability of prodrug-activating enzymes in vivo.[6,7] To minimize systemic toxicity in enzyme/prodrug cancer therapy, there is usually a time interval between the injections of enzyme and prodrug to allow for clearance of the enzyme from the circulation and normal tissue. This time interval may compromise enzyme activity because of the degradation of the enzyme in tumor intersititium by extracellular proteases such as matrix metalloproteinases (MMPs)[8] and cathepsins.[9] Therefore, increasing prodrug-activating enzyme stability in tumors is crucial for the success of enzyme/prodrug strategy. Recently, cell penetrating peptides (CPP[a]) including HIV-Tat,[10] penetratin,[11] and herpes simplex virus protein VP22[12] have attracted attention for their ability to effectively deliver conjugated therapeutic cargoes into the cytoplasm and nucleus, the most desirable loci for triggering cell death.[13] One approach to increase the therapeutic efficiency of the enzyme/prodrug strategy is to incorporate a polycationic CPP domain within the prodrug-activating enzymes. Such an approach will not only result in sustained enzymatic activity due to a shorter exposure time to extracellular proteolytic proteins but also result in the accumulation of the enzyme in the cytoplasm, leading to a high local concentration of active drug in the cytosol with an anticipated increase of therapeutic efficiency.

In our previous studies, bacterial cytosine deaminase (bCD), an enzyme that converts the nontoxic prodrug 5-fluorocytosine (5-FC) to the active antitumor drug 5-fluorouracil (5-FU), was conjugated with polycationic poly-L-lysine (PLL) labeled with biotin and multimodal imaging reporters.[14] Compared with free bCD protein, the bCD−PLL conjugate exhibited a faster internalization rate and higher enzymatic activity that increased the therapeutic efficiency in breast cancer cell cultures. In vivo fluorine magnetic resonance spectroscopy (^{19}F MRS) studies indicated that the enzymatic activity of bCD−PLL that had extravasated in human breast tumor xenografts persisted even 24 h after administration and the intratumoral 5-FC fully converted to 5-FU in about 3 h.[15] Furthermore, significant tumor growth delay and tolerable systemic toxicity were achieved when 5-FC was injected 24 h after bCD−PLL.

Here, we have examined the mechanisms underlying the sustained enzymatic stability of bCD−PLL in vivo. We hypothesized that the robust enzymatic stability of bCD−PLL may be explained in part by rapid internalization of bCD−PLL into the cytoplasm of cancer cells. This hypothesis was supported by localization of bCD−PLL in the perinuclear areas of hepatocytes as observed in immunofluorescently stained sections of the liver excised 3 h after iv injection of bCD−PLL.[15] We tested the hypothesis that cationic PLL is the principle moiety governing the efficient intracellular uptake and enhanced enzymatic stability of bCD−PLL. For comparison studies two

* To whom correspondence should be addressed. For C.L.: (address) Department of Radiology, Johns Hopkins University School of Medicine, 223 Ross Building, 720 Rutland Avenue, Baltimore, MD 21205; (phone) 410-955-6864; (fax) 410-614-1948; (e-mail) congli@mri.jhu.edu. For Z.M.B.: (address) Department of Radiology, Johns Hopkins University School of Medicine, 208C Traylor Building, 720 Rutland Avenue, Baltimore, MD 21205; (phone) 410-955-9698; (fax) 410-614-1948; (e-mail) zaver@mri.jhu.edu.

[a] Abbreviations: bCD, bacterial cytosine deaminase; PLL, poly-L-lysine; 5-FC, 5-fluorocytosine; 5-FU, 5-fluorouracil; HUVEC, human umbilical vein endothelial cell; CPP, cell permeable peptide; CPZ, chlorpromazine; MβCD, methyl-β-cyclodextrin; SEC, size exclusion chromatography; DLS, dynamic light scattering.

10.1021/jm800288h CCC: $40.75
Published on Web 06/03/2008

control bCD conjugates were synthesized. In bCD−BF the biotin and fluorophore were directly functionalized in the bCD protein while in bCD−AcPLL the positive charges in the PLL moiety were fully neutralized by acetic anhydride. The kinetics of internalization of bCD conjugates in breast cancer cell lines representing different stages of malignancy, as well as endothelial cells, was measured by flow cytometry. The mediation of cell membrane transduction by the PLL moiety of bCD−PLL was tracked by flow cytometry and confocal fluorescence microscopic imaging. Finally the enzymatic stability and therapeutic efficiency of the internalized bCD conjugates in different cell lines were evaluated. The data presented here, along with those from our earlier multimodal imaging study, provide strong evidence that a simple conjugation of PLL to bCD greatly increases the flexibility and effectiveness of this prodrug strategy in the treatment of breast cancer.

Experimental Section

Materials. All organic solvents were analytical grade from Aldrich (St. Louis, MO) and Fisher (Pittsburgh, PA) unless otherwise specified. Poly-L-lysine hydrobromide (6.0 kDa), cytosine, uracil, 5-fluorocytosine (5-FC), 5-fluorouracil (5-FU), acetic anhydride, amiloride, β-methylcyclodextrin, heparin, and streptavidin-HRP polymer were from Sigma (Milwaukee, WI). *N*-[ε-Maleimidocaproyloxy]sulfosuccinimide (Sulfo-EMCS), sulfosuccinimidyl-6-(biotinamido) hexanoate (Sulfo-NHS-LC-Biotin), *N*-succinimidyl *S*-acetylthiopropionate (SATP), EZ biotin quantitation kit, and Ellman's reagent were from Pierce (Rockford, IL). Alexa Fluor-633 succinimidyl ester, Alexa Fluor-488 labeled dextran (10 kDa), Alexa Fluor-488 labeled transferrin, and dithiothreitol (DTT) were from Invitrogen (Carlsbad, CA). The MTT cell proliferation kit was from ATCC (Manassas, VA). Amicon ultra-15 centrifugal filter tubes (5000 and 10 000 MW cutoff) were from Millipore (Bedford, MA).

Synthesis. (a) bCD−PLL. bCD conjugated PLL labeled with multimodal imaging reporters was prepared as described previously.[14] Briefly, sulfo-NHS-LC-biotin (0.78 mg, 1.4×10^{-6} mol, 8 equiv), Alexa Fluor-633 NHS ester (1.0 mg, 8.4×10^{-7} mol, 5 equiv), and DOTA-NHS ester (17 mg, 3.4×10^{-5} mol, 200 equiv) treated with PLL (1.0 mg, 1.7×10^{-7} mol) sequentially in 0.1 M HEPES, pH 8.3, provided biotin and multimodal imaging reporter labeled PLL. After complexation with Gd^{3+}, the product was further reacted with EMCS to obtain the maleimide grafted PLL. Meanwhile, bCD protein (50 mg, 1.67×10^{-7} mol) isolated from transformed *E. coli* cultures was functionalized with a sulfhydryl group. The cross-linking between maleimide of PLL and sulfhydryl of bCD generated the bCD−PLL conjugate (Figure 1A).

(b) bCD−BF. Sulfo-NHS-LC-biotin (0.73 mg, 1.3×10^{-6} mol, 8 equiv) in 50 μL of anhydrous DMF was added to bCD protein (50 mg, 1.67×10^{-7} mol, 1.67×10^{-4} M) in 1.0 mL of phosphate buffered saline (PBS), pH 7.4. After reaction for 1 h, Alexa Fluor-633 NHS ester (1.0 mg, 8.4×10^{-7} mol, 5 equiv) in 50 μL of anhydrous DMF was added, and the reaction was allowed to further proceed for 1 h. bCD−BF (Figure 1B) was purified in centrifugal filter tubes (MW 10 000 cutoff). The degree of biotin labeling was measured with the EZ biotin quantitation kit (Pierce, Rockford, IL). The ratio of Alexa Fluor-633 to bCD hexamer in bCD−BF was determined by measuring the absorbance of bCD ($\varepsilon_{279,\text{bCDmonomer}} = 76\,000\ M^{-1}\ cm^{-1}$) and Alexa Fluor-633 ($\varepsilon_{633} = 100\,000\ M^{-1}\ cm^{-1}$). The yield of bCD−BF was 92% (based on bCD hexamer).

(c) bCD−AcPLL. PLL (1.0 mg, 1.7×10^{-7} mol) in 0.1 M HEPES, pH 8.3, treated with sulfo-NHS ester-LC-biotin (0.78 mg, 1.4×10^{-6} mol, 8 equiv), Alexa Fluor-633 NHS ester (1.0 mg, 8.4×10^{-7} mol, 5 equiv), and SATP (0.25 mg, 1.0×10^{-6} mol, 6 equiv) respectively provided the biotin, fluorophore, and thioacetate conjugated PLL **2**. Treatment of **2** with excess acetic anhydride (3.5 mg, 3.4×10^{-5} mol, 200 equiv) in methanol resulted in the full acetylation of remaining amines in **2**, generating **3**. The number of primary amines in PLL before and after acetylation was determined by the 2,4,6-trinitrobenzenesulfonic acid (TNBSA) assay according to the manufacturer's protocol (Pierce, Rockford, IL). Reduction of **3** in hydroxylamine gave **4** with deprotected sulfhydryl moiety. bCD (50 mg, 1.67×10^{-7} mol, 1.67×10^{-4} M) was treated with EMCS (0.31 mg, 1.0×10^{-6} mol, 6 equiv) in PBS, pH 7.4, generating compound **5** with maleimide group. The cross-linking between **4** and **5** offered the bCD−AcPLL (Figure 1C), which was purified by the centrifugal filter tube (MW 10 000 cutoff) with a yield of 87% (based on bCD hexamer).

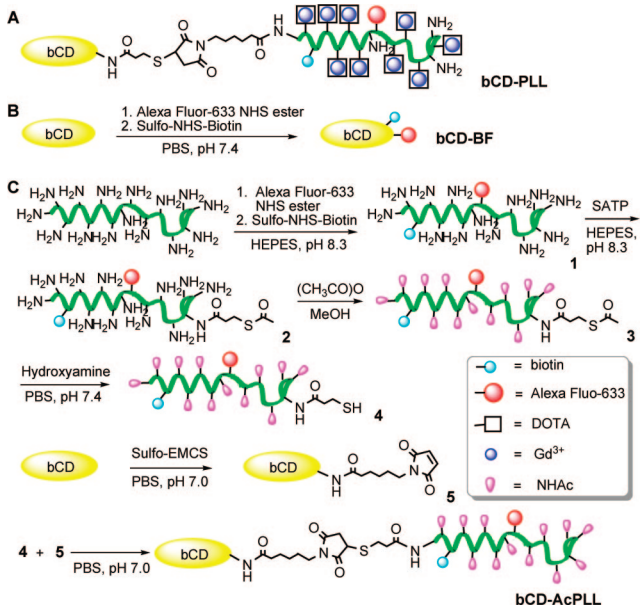

Figure 1. Preparation of bCD conjugates: (A) schematic representation of bCD−PLL;[14] (B) synthetic procedure of bCD−BF; (C) synthetic procedure of bCD−AcPLL.

Characterization. (a) Determining Molecular Weight of bCD Conjugates. The molecular weights of bCD conjugates were estimated on a Waters Ultrahydrogel 500 (7.8 mm × 300 mm) size-exclusion column, which was operated by the high performance liquid chromatography (HPLC) system equipped with Waters 1525 binary pump and Waters 2487 dual wavelength absorbance detector (Waters Inc., Milford, MA). Typical HPLC parameters were as follows: mobile phase, 0.1 × PBS, pH 7.4; isocratic flow rate, 0.7 mL/min; operating temperature, 25 °C; injected volume, 20 μL. Elutions were monitored at 280 and 633 nm in separate experiments.

(b) Determining the Size of bCD Conjugates. Hydrodynamic radii and size distributions of bCD conjugates were determined on Zetasizer Nano Zen3690 (Malvern Instruments, Southborough, MA) dynamic light scattering (DLS) system equipped with a He−Ne laser (633 nm, 4 mW). The instrument was calibrated with a standard solution of 2 mg/mL bovine serum albumin (BSA). The bCD conjugates were diluted into PBS, pH 7.4, to a concentration of 1.0 mg/mL and filtered through a 0.22 μm filter. Calculations were done with the regularization algorithm provided by DYNAMICS software.

(c) Strepavidin Based ImmunoBlot-like Analysis. bCD conjugates with the same calculated molar biotin concentrations were denatured by 1:1 dilution in 2× treatment buffer [200 mM Tris, pH 6.8, 4% (w/v) sodium dodecyl sulfate (SDS), 24% (v/v) glycerol, 0.01% (w/v) bromphenol blue, and 5% (v/v) 2-mercaptoethanol (BME)] and heated 15 min at 70 °C. bCD−PLL (10 ng), bCD−BF (7.0 ng), and bCD−AcPLL (10 ng) were resolved on a 12% SDS gel and transferred to polyvinylidene difluoride membranes (Immobilon PVDF, Millipore, Bedford, MA). Membranes were blocked in PBS with 1% BSA and 0.05% (v/v) Tween-20 for 1 h, washed 2× in PBS with 0.05% (v/v) Tween-20, and then incubated in a 1:1000 dilution of streptavidin−HRP in PBS with 0.05% (v/v) Tween-20 for 1 h. Following washing 6× in PBS with 0.05% Tween-20, blots were developed using a SuperSignal West Pico

chemiluminescent kit (Pierce, Rockford, IL) and protein bands were visualized on X-ray film (Kodak Biomax, Kodak, Rochester, NY).

(d) Fluorescence Electrophoresis Imaging. Similar to strepavidin blots, bCD conjugates (5.0 μg) were denatured in sample treatment buffer and subsequently loaded onto 12% SDS−PAGE gel. After electrophoresis, fluorescent and bright-field images of the resulting polyacrylamide gels were acquired by a Xenogen IVIS imaging system 200 series (Caliper, Hopkinton, MA) small animal optical imager equipped with a Cy5.5 excitation and emission filter set using the following settings: FOV = 12.8 cm, *f*/stop = 4, bin = high resolution, exposure time = 5 s.

Enzymatic Kinetics and Specific Activity. Kinetic values of the bCD conjugates with cytosine or 5-FC as substrate were performed according to a previously reported method.[14] Briefly, bCD and bCD conjugates were added to the substrate with selected concentrations in 50 mM Tris-HCl, pH 7.5. Initial velocities were calculated from changes in absorbance values obtained at 286 nm for cytosine and 297 nm for 5-FC and the corresponding known changes in molar absorbance coefficients ($\Delta\varepsilon_{286\text{-cytosine}} = -0.68$ mM^{-1} cm^{-1}; $\Delta\varepsilon_{297\text{-5-FC}} = -0.41$ mM^{-1} cm^{-1}). Woolf plots were used to determine Michealis constants (K_m), turnover number k_{cat} ($k_{cat} = V_{max}/[E]$, where V_{max} is the maximal catalytic velocity and [E] is the total enzyme concentration), and catalytic efficiency (k_{cat}/K_m) of bCD conjugate. The specific activity of bCD conjugates was calculated as follows:

$$U = \frac{[\Delta C_{susbstrate}][V]}{[T][W_{enzyme}]} \quad (1)$$

where U is enzymatic activity with a unit of (μmol/min)/mg, $[\Delta C_{substrate}]$ is the change in cystosine/5-FC concentration (mM), $[V]$ is volume (mL), $[T]$ is the reaction time (min), and $[W_{enzyme}]$ is the total enzyme weight (mg).

Cell Culture. Three human mammary epithelial cell (HMEC) lines representing different stages of malignancy were obtained from the American Type Culture Collection (ATCC, Rockville, MD). MCF-12A, a spontaneously immortalized nontumorigenic breast epithelial cell line was cultured in DMEM-Ham's F12 medium (Invitrogen) supplemented with 10% horse serum, 100 U/mL penicillin, and 100 μg/mL streptomycin (Pen/strep), epidermal growth factor (20 mg/mL), cholera toxin (100 ng/mL), insulin (10 ng/mL), and hydrocortisone (500 ng/mL). MCF-7, a breast cancer cell line that exhibits low tumorigenicity, was cultured in EMEM medium (Mediatech, Herndon, VA) supplemented with 10% fetal bovine serum (FBS) and pen/strep. The highly malignant MDA-MB-231 cell line was maintained in RPMI-1640 medium (Invitrogen) supplemented with 10% FBS and pen/strep. The human umbilical vein endothelial cell (HUVEC) line purchased from Cambrex (Walkersville, MD), sixth generation or less, was cultured in EGM-2 media supplemented with SingleQuot Kits (Cambrex) in accordance to the manufacturer's instructions. All the cells were cultured as monolayers in 75 cm^2 culture flasks in a standard incubator maintained with a humidified atmosphere of 5% CO_2 in air at 37 °C.

Flow Cytometric Analysis. For the kinetic and concentration-dependent internalization studies, cells grown in 60 mm plates were treated with bCD conjugates. At the end of treatment, cells were washed 3× with PBS, trypsinized, then washed again with PBS. The cell pellet after centrifugation was resuspended in 0.6 mL of 0.5% paraformaldehyde (PFA) and stored at 4 °C until analysis. For the heparin blocked internalization, cells were preincubated with 10 μg/mL heparin for 30 min and then with 100 μg/mL bCD−PLL for 2 h in the presence of 10 μg/mL heparin. Finally, the cells were washed and fixed as described before. For the temperature-dependent internalization, cells were treated with 100 μg/mL bCD−PLL for 30 min at 4 and 37 °C. At the end of incubations, cells were washed with ice-cold PBS for 3× prior to harvest and fixation. Flow cytometry was performed using a FACS Calibur instrument (Becton Dickinson, San Jose, CA) equipped with a 633 nm He−Ne laser. Then 5000 evens per sample were analyzed. CellQuest 3.3 software (BD Bioscience) was used for data acquisition and analysis.

Confocal Laser-Scanning Fluorescence Microscopy. All fluorescence microscopic images were performed with a Zeiss LSM 510 META confocal laser-scanning microscope (Carl Zeiss, Inc., Thornwood, NY) using a Plan-Apochromat 63×/1.4 oil immersion lens (Zeiss). All bCD conjugates were excited with a He−Ne laser (633 nm), and fluorescence of conjugated Alexa Fluor-633 was detected by a photomultiplier tube using a 650 nm long pass filter. The Alexa Fluor-488 labeled dextran or transferrin was excited with an Ar laser (488 nm), and fluorescence was detected by a secondary photomultiplier by applying a 505−550 nm band-pass filter.

Uptake and Intracellular Distribution of bCD Conjugates in Live Cells. To avoid artifacts that occur during fixation, all the confocal microscopic experiments were conducted in live cells. Cells (2×10^4) cultured on 35 mm glass bottom culture dishes (14 mm microwell, MatTek, Ashland, MA) to approximately 80% confluence were incubated with 200 ng/mL bCD conjugate in 2 mL of media supplemented with 10% FBS for 30 min at 37 °C. At the end of incubation, the cells were washed with Hanks balance salt solution (HBSS) 3× prior to addition of 1 mL of phenol red free media, and the cells were immediately imaged by confocal fluorescence microscopy.

Determination of Internalization Pathway of bCD−PLL. (a) Colocalization between bCD−PLL and Transferrin. MDA-MB-231 cells were simultaneously incubated with 100 ng/mL Alexa Fluor-488 labeled transferrin and 200 ng/mL bCD−PLL in 2 mL of serum free medium for 30 min at 37 °C. The cells were washed 3× with HBSS, and 1 mL phenol red free medium supplemented with 10% FBS was added prior to microscopic analysis.

(b) Colocalization between bCD−PLL and Dextran. MDA-MB-231 cells were treated with 0.1 mg/mL Alexa Fluor-488 labeled dextran (10 kDa) at 37 °C for 3 h. After the sample was washed with HBSS, culturing was continued in dextran free medium for 16 h to facilitate labeling of lysosomes with the probe.[16] To minimize recycling labeling events, media were changed and cells were treated with 200 ng/mL bCD conjugates for 30 min at 37 °C prior to the microscopy studies.

(c) Colocalization between bCD−PLL and Transferrin in Presence of Endocytosis Inhibitor. MDA-MB-231 cells were pretreated for 30 min (with the exception of amiloride treatment of 15 min) in serum free medium with the following drugs: 10 μM chlorpromazine, 5 mM methyl-β-cyclodextran, or 5 mM amiloride. Media were removed, and fresh media containing 200 ng/mL bCD−PLL as well as the corresponding inhibitor were added. After incubation for an additional 30 min, cells were washed with HBSS, and phenol red free media was applied prior to immediate fluorescence microscopy. Colocalization coefficients were measured by the ImageJ software (NIH) with Colocalization Finder plugin (threshold: 50%).

Enzymatic Stability of Internalized bCD−PLL in Cell Cultures. Cells were seeded into 96-well plates with densities of 5×10^2 to 1×10^4 cells/well. Upon attachment, cells were incubated with increasing concentrations (0.2−100 μg/mL) of bCD conjugate in media supplemented 10% FBS for 30 min at 37 °C. Then cells were washed 2× with HBSS prior to addition of 100 μL of fresh medium supplemented with 10% serum. The cells were further incubated at 37 °C for 0, 6, or 24 h. Next, 5-FC (1.5 mM, final concentration) was added, and the cells were further incubated for 90 h at 37 °C in 5% CO_2. At the end of incubation, 100 μL/well of phenol red free medium and 10 μL of MTT were added to each well, and the plate was incubated for 4 h at 37 °C in 5% CO_2. After addition of 100 μL of detergent regent (ATCC), the plates were kept in the dark overnight at room temperature, and an absorbance reader (PerkinElmer, 1420 VICTOR^3 V multilabel counter, Waltham, MA) was used to measure the absorbance in each well at 570 and 650 nm. The average values from the eight replicates were calculated, and the cell viabilities were determined as previously described.[14]

Statistics. Values are presented as the mean ± SD of at least three experiments. We analyzed statistical differences by Student's

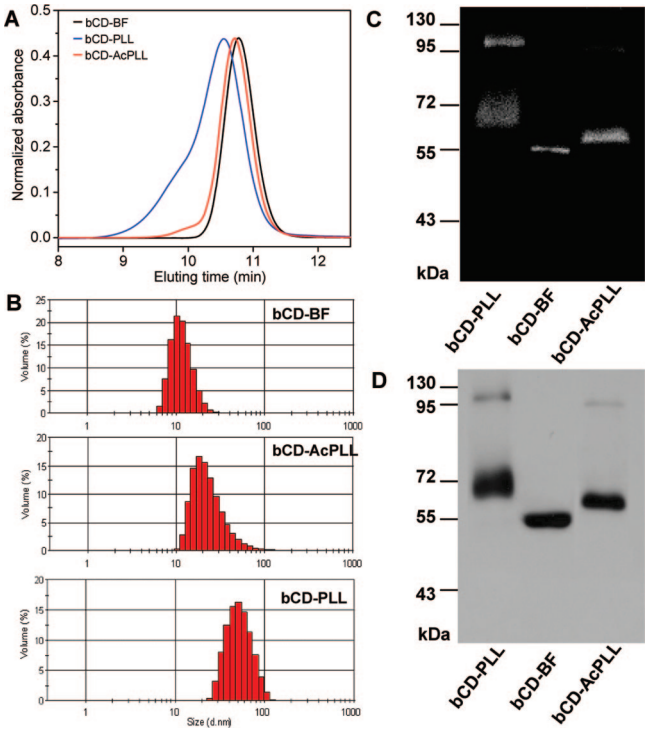

Figure 2. Characterization of bCD conjugates: (A) normalized gel permeable chromatography of bCD−PLL (blue line), bCD−BF (black line), and bCD−AcPLL (red line) monitored at 280 nm; (B) hydrodynamic radii and size distribution of bCD conjugates measured by DLS; (C) representative fluorescent image of a denatured SDS−PAGE gel loaded with the indicated bCD conjugates (5 μg protein/well); (D) strepavidin-based blot analysis of bCD conjugates. bCD conjugates were loaded with the same biotin molar number.

t-test (Excel 2002, Microsoft). Statistical significance was defined at the level of $P < 0.05$ (two-tailed).

Results

Synthesis and Characterization of bCD Conjugates. The schematic of bCD−PLL and the synthetic procedures for bCD−BF and bCD−AcPLL are illustrated in Figure 1. bCD−PLL was synthesized as previously described.[14] bCD−BF was prepared by direct modification of biotin and fluorophore on the bCD protein. In bCD−AcPLL, to completely neutralize the positive charges in PLL moiety, biotin, fluorophore, and *S*-acetylthiopropionate were grafted on PLL before its acetylation with excess acetic anhydride. A TNBSA assay demonstrated that the number of free amines in PLL moiety decreased from 32 to 1 after the acetylation. Determination of the molar ratios of bCD hexamer/PLL/fluorophore/biotin in bCD−PLL and bCD−AcPLL indicated the identical value of 1/1/0.9/2, and the molar ratio of bCD hexamer/fluorophore/biotin in bCD−BF was 1/0.8/3.

The molecular weight (MW) of bCD conjugates was determined by size-exclusion chromatography (SEC) (Figure 2A). The superimposed peaks monitored at 280 nm (bCD protein) and 635 nm (Alexa Fluor-633) confirmed covalent conjugation between PLL and bCD (data not shown). The MWs of bCD−PLL, bCD−BF, and bCD−AcPLL were measured as 345, 302, and 325 kDa, respectively, by applying the elution volume/void volume (V_e/V_o) value in conjunction with the protein calibration curve of SEC column.[14] DLS measurements gave the hydrodynamic and size distribution pattern of bCD conjugates in PBS. Mean hydrodynamic radii of bCD−PLL, bCD−BF, and bCD−AcPLL were determined as 24.4, 11.8, and 12.4 nm (Figure 2B), respectively. The molecular structure of bCD conjugates was further evaluated by fluorescence imaging of denatured proteins resolved in SDS−PAGE gels (Figure 2C) and streptavidin based blots of such gels (Figure 2D). In fluorescence images, both bCD−PLL and bCD−AcPLL exhibited two fluorescent bands with apparent MWs of 70 and 115 kDa and of 60 and 97 kDa, respectively; a single fluorescent band at approximately 55 kDa was observed for bCD−BF. As shown in Figure 2D, a similar band distribution pattern was observed in the strepavidin blot analysis. Since pure bCD is obtained from the *E. coli* cultures and no other bacterial proteins contaminate these preparations, only bCD conjugates were detected on these gels.

Table 1. Kinetic Parameters of bCD and bCD Conjugates[a]

	cytosine (5-fluorocytosine)[b]			
	K_m (mM)	k_{cat} [d] (s^{-1})	k_{cat}/K_m (mM^{-1} s^{-1})	specific activity (μmol min^{-1} mg^{-1})
bCD[c]	0.19(3.9)	185(71)	973(18)	144[e](58)[f]
bCD−BF	0.19(4.0)	183(70)	963(18)	134[e](56)[f]
bCD−PLL[c]	0.16(3.7)	148(74)	925(20)	121[e](61)[f]
bCD−AcPLL	0.16(3.8)	150(74)	937(19)	125[e](62)[f]

[a] Mean values of duplicate determinations in 50 mM Tris buffer, pH 7.5, at 25 °C. Protein concentrations were calculated from absorbance of bCD monomer (ε_{279} = 76 mM^{-1} cm^{-1}). [b] The values in parentheses represent the parameters when 5-FC was used as a substrate. [c] The data presented here are from our previous communication.[14] [d] k_{cat} values were calculated using the equation $k_{cat} = V_{max}/[E]$. [e] Determined in 0.5 mM cytosine. [f] Determined in 9.6 mM 5-FC. See Experimental Section for details.

Enzyme Kinetics. As shown in Table 1, bCD−PLL and bCD−AcPLL exhibited a similar enhancement in K_m as well as a small decrease in k_{cat} relative to native bCD when cytosine was used as substrate. The decrease in k_{cat} caused a small decrease in catalytic efficiencies (k_{cat}/K_m values) and specific activities for these two conjugates with this substrate. In contrast, the kinetics of bCD−BF with cytosine as substrate was unchanged relative to bCD. All bCD conjugates exhibited similar kinetics when 5-FC was the substrate (Table 1). Thus, in vitro activity of bCD with 5-FC was unchanged regardless of any modifications but bCD−PLL and bCD−AcPLL conjugates exhibited about a 5% lower turnover number and 10% lower specific activity with cytosine as substrate.

Kinetics of Internalization of bCD Conjugates. The cellular internalization kinetics of bCD−BF, bCD−PLL, bCD−AcPLL in human breast MDA-MB-231 cancer cells are shown in Figure 3A,B. The bCD conjugates (100 μg/mL) in serum free media were added to the cells, and the cellular fluorescence was quantitatively assessed at selected time points by flow cytometry after washing with trypsin to remove any nonspecific bound conjugate on the cell surface. Analysis of the flow cytometry profiles (upper profile of Figure 3A) and time-dependent cellular fluorescence values (large plot of Figure 3B) clearly indicates that the cellular uptake of bCD−PLL rapidly increased in a nearly linear manner during the first 16 h, which was followed by a slow and progressive increase and an apparent plateau from 30 to 48 h. In contrast, as shown in the lower profiles of Figure 3A and the inset of Figure 3B, 80% uptake of bCD−BF and bCD−AcPLL was already complete in the first 2 h and the mean cellular fluorescence increased slightly over the following 24 h incubation. All three bCD conjugates were internalized within MDA-MB-231 cells, but bCD−PLL demonstrated an average cellular fluorescence that was 45−50 times higher than that of bCD−BF or bCD−AcPLL. Consistent with the flow cytometry results, confocal fluorescence microscopic imaging revealed a much stronger intracellular fluorescence signal from bCD−PLL

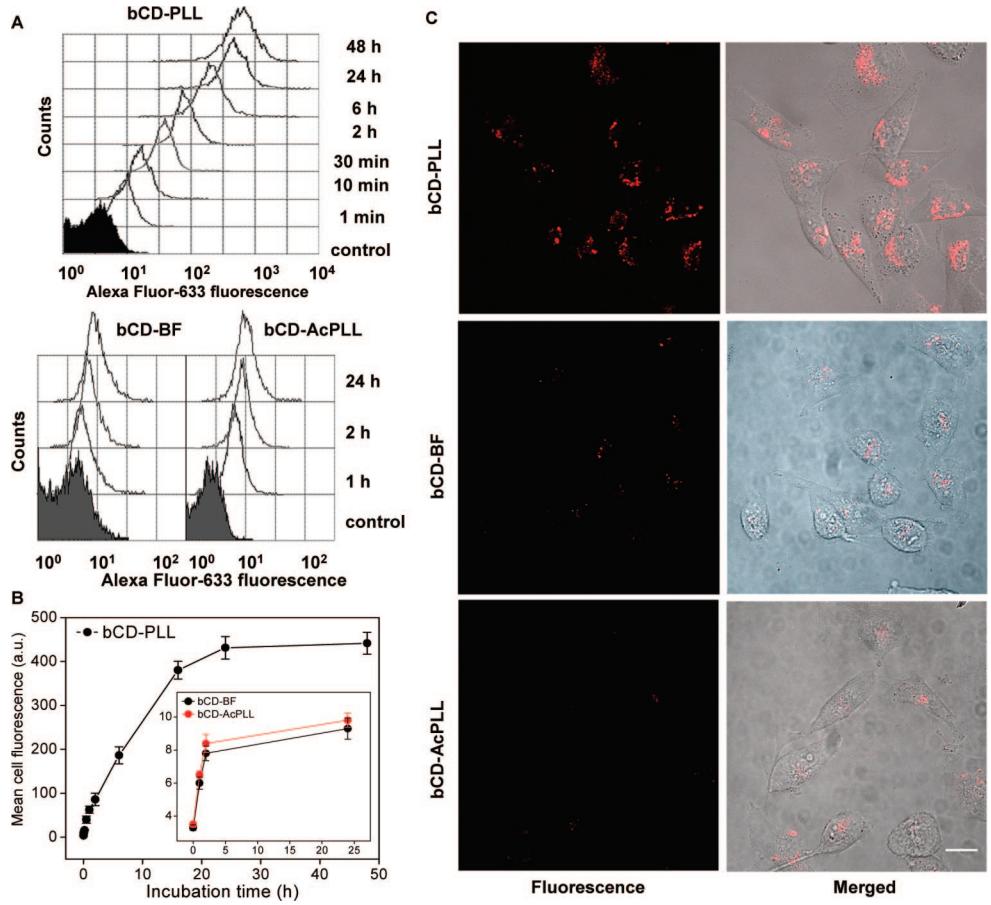

Figure 3. Kinetics of internalization of bCD conjugates in live human breast MDA-MB-231 cancer cells. (A) The cells were incubated with 100 μg/mL bCD−PLL, bCD−BF, or bCD−AcPLL for selected periods of time as indicated, and then cell fluorescence was analyzed by flow cytometry. The filled peaks show autofluorescence of cells before the treatment. (B) Mean fluorescence intensities of cells were analyzed by flow cytometry after incubation with bCD−PLL (100 μg/mL) for the indicated periods. Inset is time-dependent fluorescence intensities of cells treated with bCD−BF or bCD−AcPLL (100 μg/mL). Experiments were performed in triplicate, and values represent the mean ± SD. (C) Fluorescence and fluorescence/phase contrast (PC) merged confocal microscopic images of live cells after the treatment of 200 ng/mL bCD conjugate for 15 min at 37 °C. All images were obtained under the same instrumental conditions: scale bar, 15 μm.

(top panel of Figure 3C) than bCD−BF and bCD−AcPLL (middle and bottom panels of Figure 3C) in live MDA-MB-231 cells under the same experimental conditions. Thus these data unambiguously demonstrated that the internalization of bCD−PLL was much higher than either of the other two bCD conjugates.

Highly Malignant Breast Cancer Cells Were Most Efficient at Internalizing bCD−PLL. To determine if the high capacity of bCD−PLL internalization was unique to highly malignant MDA-MB-231 cells, bCD−PLL uptake was also investigated in weakly tumorigenic MCF-7 breast cancer cells, nontumorigenic immortalized breast epithelial MCF-12A cells, and human umbilical vein endothelial cells (HUVEC). Confocal fluorescence images of these four cell lines after incubation with bCD−PLL (200 ng/mL) for 30 min are shown in Figure 4A. bCD−PLL was taken up by all the cell lines, and the fluorescence appeared to be predominantly located within perinuclear areas with little or no fluorescence near the periphery or at the cells surface. Interestingly, enlargement of the images (Figure 4B) revealed that the size of fluorescent vesicles appeared to depend on the cell type. Quantitative measurements indicated that the mean vesicular size in the cancer cell lines was significantly larger than in the nonmalignant epithelial cell line and the HUVEC (Figure 4C). The average vesicular diameter of MCF-7, MDA-MB-231, HUVEC, and MCF-12A were measured as 2.4, 2.1, 1.1, and 0.3 μm, respectively. The uptake of bCD−PLL in different cell lines was further quantitatively analyzed by flow cytometry. As shown in Figure 4D, following a 2 h incubation with bCD−PLL, MDA-MB-231 cells showed 2-, 3-, and 5-fold higher fluorescent intensity compared to HUVEC, MCF-7, and MCF-12A, respectively.

Transduction of bCD−PLL into Cultured Cells Is Energy-Dependent, Blocked by Heparin, and Unaffected by Serum. The highly efficient internalization of bCD−PLL prompted us to study its transduction mechanism in cell culture. To test whether internalization was mediated through energy-dependent endocytosis versus passive diffusion, cellular uptake of bCD−PLL was quantified by flow cytometry at both 4 and 37 °C because most cellular activities are essentially arrested at 4 °C. As shown in Figure 5A, uptake of bCD−PLL in all four cell lines is an energy-dependent process, which dramatically decreased at 4 °C compared to that at 37 °C. Additional evidence against unlimited passive diffusion of bCD−PLL into cells is shown in the insert of Figure 5B, which demonstrates that the transduction of bCD−PLL into MDA-MB-231 cells at 37 °C was saturated at high bCD−PLL concentrations. Meanwhile, symmetric and narrow cellular fluorescence profiles shown in Figure 5B suggest a homogeneous uptake of bCD−PLL in cells. Polyanionic heparin has been shown to block the transduction of TAT-fused proteins by competently binding with polycationic CPPs.[17] To confirm that transduction was mediated by the polycationic characteristic of PLL, we compared the uptake efficiency of

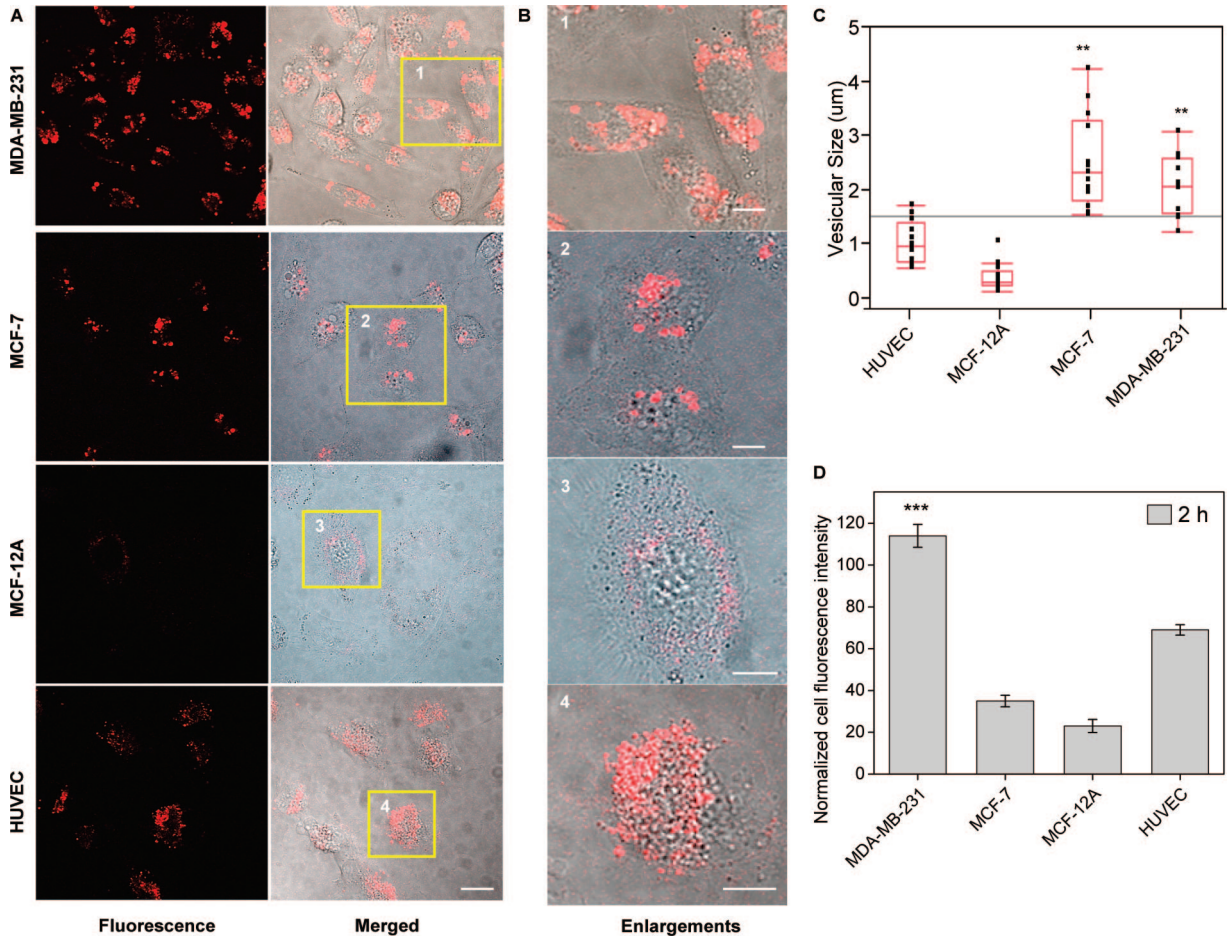

Figure 4. Cellular uptake of bCD−PLL into different cell lines. (A) Fluorescence and fluorescence/phase contrast merged confocal microscopy images of live HMECs and HUVECs treated with 200 ng/mL bCD−PLL for 30 min at 37 °C: scale bar, 15 μm. (B) Enlargements of corresponding image areas highlighted by a square in panel A. The scale bars represent 5 μm. (C) Quantification of the diameter of fluorescent vesicles in the cytoplasm of 25−30 randomly selected cells from three independent experiments following incubation with 200 ng/mL bCD−PLL: (**) $P < 0.01$, compared with MCF-12A cells. (D) Flow cytometry analysis of mean fluorescence of various cell lines treated with 100 μg/mL bCD−PLL for 2 h at 37 °C. Experiments were performed in triplicate, and values represent the mean ± SD: (***) $P < 0.001$, compared with MCF-12A cells.

bCD−PLL into MDA-MB-231 cells in the absence and presence of 10 μg/mL heparin. Figure 5C shows that heparin inhibited bCD−PLL uptake by a factor of 20−55% after incubation for 1−6 h at 37 °C, which is further evidence that the positive charge of the PLL moiety is necessary for efficient uptake. On the other hand, no significant change in the cellular uptake of bCD−PLL (10, 50, and 100 μg/mL) was observed in the presence or absence of 10% FBS (Figure 5D). Taken together, these results indicate that efficient transduction of bCD−PLL into cells is an energy-dependent process that is mediated in part by the polycationic character of the PLL moiety but is independent of serum components.

bCD−PLL Is Internalized through a Clathrin-Mediated Endocytosis Pathway. To clarify the trafficking pathway and intracellular destination of bCD−PLL in cell culture, bCD−PLL and Alexa Fluor-488 labeled transferrin, a widely used fluorescent marker for clathrin-mediated endocytosis,[18] were mixed and added to the cultured live MDA-MB-231 cells. As indicated in Figure 6A, most of the bCD−PLL and transferrin appeared to colocalize in discrete cytoplasmic vesicles as indicated by the yellow color from the merged image (Figure 6A and Figure 6F1). Notably, single transferrin labeled vesicles in green were also found in the periphery of MDA-MB-231 cells after incubation for 30 min (Figure 6F1). The involvement of clathrin-mediated endocytosis in the internalization of bCD−PLL was further verified by the remarkably reduced uptakes of both bCD−PLL and transferrin in cells pretreated with chlorpromazine (CPZ), a clathrin inhibitor that disrupts the assembly of the clathrin adaptor protein at the cell surface.[19] Cells treated with CPZ exhibited little or no internalization of either bCD−PLL or transferrin (Figure 6B and Figure 6F2). We next tested the possibility that lipid raft-mediated macropinocytosis[20] or lipid raft-mediated caveolar endocytosis[21] might contribute to bCD−PLL internalization. Thus, MDA-MB-231 cells were pretreated with amiloride, a drug that restricts lipid raft-mediated macropinocytosis by inhibiting Na^+/H^+ exchange protein in the plasma membrane,[22] and the treatment was followed with bCD−PLL and transferrin incubation. Figure 6C and Figure 6F3 indicate that colocalization between the bCD−PLL and transferrin was not affected by the presence of amiloride. Additionally, cells were pretreated with methyl-β-cyclodextrin (MβCD), a drug that extracts cholesterol from cell membranes, thus disrupting lipid rafts required in the caveolar endocytosis.[23] As shown in Figure 6D, the colocalization between transferrin and bCD−PLL is independent of the presence of MβCD. Clathrin-mediated endocytosis is known to proceed through endosome maturation and eventual to fuse with lysosomes.[24] Therefore, we tested the possible colocalization between bCD−PLL and Alexa fluo-488 labeled dextran (10 kDa), a long-term lysosomal marker in live cells.[16] As seen in Figure 6E and Figure 6F4, an obvious colocalization was demonstrated between bCD−PLL and dextran in live MDA-MB-231 cells.

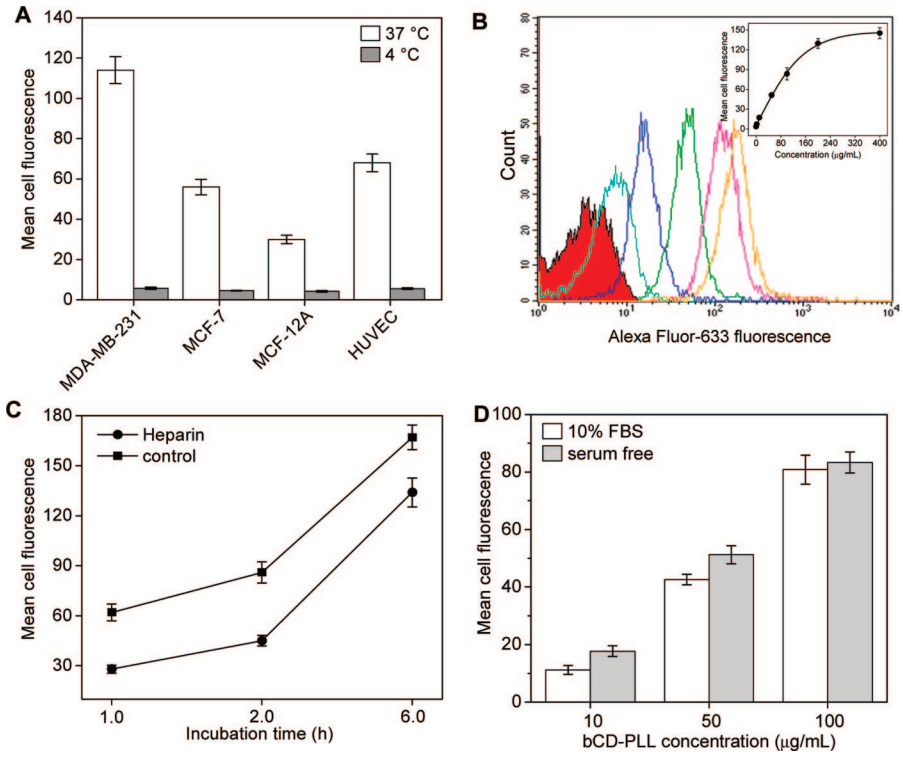

Figure 5. Conditional internalization of bCD−PLL in MDA-MB-231 cells. (A) Mean fluorescence of cells analyzed by flow cytometry after treatment with 100 μg/mL bCD−PLL for 2 h at 37 and 4 °C. (B) Flow cytometry histograms of cells treated with bCD−PLL with various concentrations (2−200 μg/mL) in serum free media for 1.0 h. Inset is a plot of concentration dependent mean cell fluorescence intensity. (C) Mean fluorescent intensities of cells after incubation with bCD−PLL (100 μg/mL) for 1.0, 2.0, and 6.0 h in serum free media supplemented with 10 μg/mL heparin. (D) Mean fluorescent intensities of cells after incubation with bCD−PLL (10, 50, and 100 μg/mL) in serum free or 10% FBS supplemented medium for 1.0 h at 37 °C. Experiments were performed in triplicate, and values represent the mean ± SD.

A plot of the colocalization coefficients versus drug treatment (Figure 6G) demonstrates that the colocalization coefficients between bCD−PLL and transferrin or dextran (shown in Figure 6A−F) were about 75% except in cells pretreated with the clathrin inhibitor CPZ.

Internalized bCD−PLL Demonstrated High Enzymatic Stability in Cell Cultures. We next studied the enzymatic stability of internalized bCD conjugates in cell cultures. In a typical experiment, after the enzyme internalization, the medium was changed and cells were washed to remove any extracellular conjugate. Therefore, prodrug added was only converted by the internalized bCD conjugate. As shown in Figure 7A,B, internalized bCD−PLL maintained high enzymatic activity in both cancer cell lines. Treatment of containing internalized bCD−PLL with 5-FC resulted in cell viability as low as that of cells treated with 5-FU alone. The cytotoxicity increased with the concentration of bCD−PLL used. This result correlated well with the concentration-dependent cellular uptake of this conjugate demonstrated in Figure 5B. Noticeably, moderate cell growth inhibition (>30%) was demonstrated even at the lowest concentration (0.2 μg/mL) of this conjugate. More importantly, these data demonstrate that bCD−PLL retained high enzymatic stability in the cytoplasm. Compared with cells treated with 5-FC immediately after uptake of the enzyme, only a slightly less cytotoxicity was observed when the prodrug was added 24 h after internalization of bCD−PLL (Figure 7A,B). Interestingly, HUVEC and MCF-12A cells exhibited vastly different chemosensitivity to 5-FU in control experiments. The relative viabilities of HUVEC and MCF-12A cells were recorded as 62% and 4%, respectively, after treatment with 5-FU alone (Figure 7C and Figure 7D) compared to 20% in the case of cancer cells. Internalized bCD−PLL alone demonstrated minimal cytotoxicity in all four cell lines (Figure 7E). Significantly, both HUVEC and MCF-12A cells showed higher survival rates compared to cancer cells when 5-FC was added 24 h after internalization of bCD−PLL (100 μg/mL), which likely reflects the low enzyme uptake of MCF-12A cells and the lack of sensitivity of HUVECs to 5-FU (Figure 7E). Figure 7F showed the cytotoxicity induced by internalized bCD conjugates upon treatment with 5-FC. Like bCD−PLL, both bCD−BF and bCD−AcPLL alone demonstrated minimal cytotoxicity to MDA-MB-231 cells. Consistent with their low internalization, these conjugates exerted only a marginal therapeutic effect compared to bCD−PLL.

Discussion

Among the various enzyme/prodrug combinations developed, the bCD/5-FC strategy was chosen because of the high enzymatic stability of bCD and its unique bystander effect, in which the active drug 5-FU is readily transported between cells by facilitated diffusion, inducing cytotoxicity in neighboring cancer cells.[25] The advantages of PLL include its biodegradability and extended coil conformation that may facilitate its extravasation into tumor interstitium.[26] Importantly, the modification of functional groups in the PLL moiety prior to conjugating it with bCD does not compromise enzymatic activity. We recently demonstrated that conjugation of PLL labeled with biotin and multimodal imaging reporters with bCD had little affect on bCD function in vitro and in vivo.[14,15]

Data obtained in the current study demonstrate a key advantage that, relative to bCD, the grafted PLL moiety imbues the enzyme with greater cellular internalization efficacy resulting in higher therapeutic efficacy of the enzyme/prodrug strategy. In our study, bCD−PLL and two control conjugates, bCD−BF

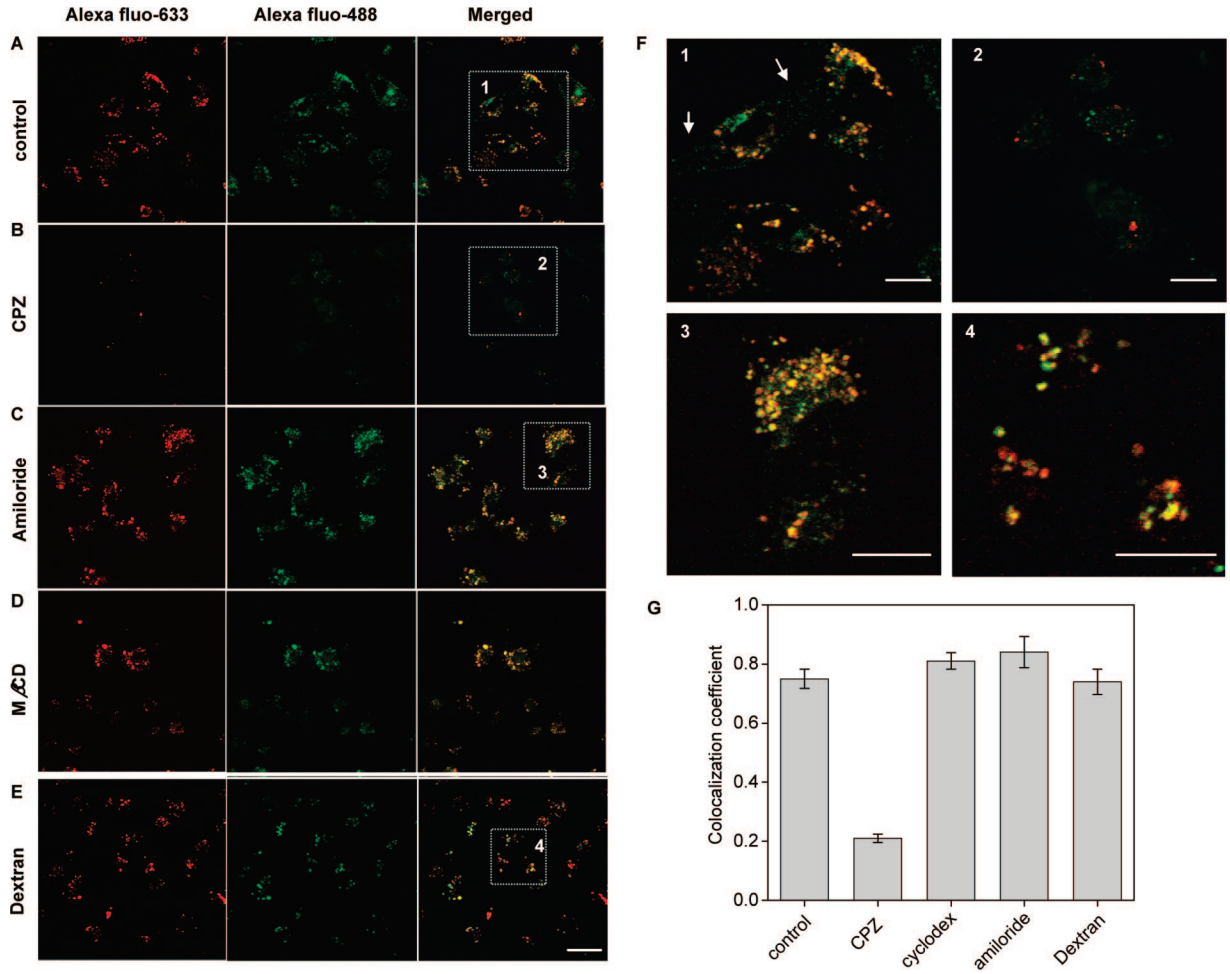

Figure 6. bCD−PLL is internalized into live MDA-MB-231 cell through clathrin-mediated endocytosis. (A) Representative confocal fluorescence microscopic images of live cells after the treatment of 200 ng/mL bCD−PLL and 100 ng/mL Alexa fluo-488 labeled transferrin (Tf). The fluorescence of Alexa Fluor-633 is shown in red, and Alexa fluo-488 is displayed in green. The yellow color represents the colocalization between bCD−PLL and Tf. Scale bar, 20 μm. (B−D) Representative fluorescence microscopic images of live cells pretreated with 10 μg/mL chlorpromazine (CPZ) (B), 5 mM amiloride (C), and 5 mM methyl-β-cyclodextrin (D) for 30 min (amiloride for 15 min) prior to the incubation with 200 ng/mL bCD−PLL and 100 ng/mL Alexa Fluor-488 labeled Tf for 15 min in media supplemented with 10% FBS. (E) Representative images of live cells pretreated with 100 μg/mL Alexa Fluor-488 labeled dextran for labeling lysosomes before incubation with 200 ng/mL bCD−PLL as described in the Experimental Section. The fluorescence of Alexa Fluor-633 was displayed in red, and Alexa Fluor-488 was displayed in green. The yellow color represents colocalization. (F) Enlargements of corresponding image areas highlighted by a square in merged panels A, B, C, and E. Arrows point out the Tf single stained vesicles at the periphery of the cell. The scale bars present 10 μm. (G) Colocalization coefficients of the bCD−PLL fluorescence with Tf or dextran fluorescence in live cells after the treatments described in panels A−E. Six randomly selected images were analyzed. Data are expressed as the mean ± SD.

and bCD−AcPLL, were synthesized and well characterized by SEC, DLS, denatured SDS−PAGE, and biotin/streptavidin blot analysis. SEC demonstrated that the molecular weight of the bCD conjugates was close to calculated values. The finding with DLS that bCD−PLL has a much larger hydrodynamic size than bCD−AcPLL (24.4 nm vs 14.4 nm) may partially be explained by the multiple water molecule layers surrounding the Gd^{3+}-DOTA chelates labeled in the PLL moiety.[27] Similar band distribution patterns obtained in fluorescent images of SDS−PAGE gel and complementary biotin/streptavidin based blotting further clarify the degree of modification of the bCD conjugates. A single band of bCD−BF with a MW of 55 kDa was identified as the bCD monomer (~51 kDa) modified with fluorophore and biotin. Similarly, the majority of denatured bCD−PLL and bCD−AcPLL migrating at apparent MWs of 70 and 60 kDa, respectively, were characterized as bCD monomers functionalized with a single PLL moiety with different degrees of labeling. The two slower migrating bands at apparent MWs of 115 and 100 kDa for bCD−PLL and bCD−AcPLL, respectively, were best identified as bCD dimers that were conjugated with a single PLL moiety. The phenomenon of band broadening of bCD−PLL was explained by the nonidentical size of PLL and a heterogeneous degree of labeling of Gd^{3+}-DOTA chelates in the conjugated PLL moiety. Compared to free bCD protein, three bCD conjugates demonstrate similar kinetic parameters such as K_m, k_{cat}, and k_{cat}/K_m to the substrates of cytosine and 5-FC, which confirms that a singly conjugated PLL moiety does not compromise the enzymatic activity. In bCD−PLL and bCD−AcPLL, bCD hexamer and PLL moiety were conjugated through a flexible cross-linker that is about 15 nm in length. The extended linker may keep the PLL moiety away from the active center of the enzyme, resulting in an intact enzymatic activity during the conjugation process.

A comparison of the internalization kinetics of three bCD conjugates clearly indicates that positive charges in PLL moiety function in a crucial role in accelerating the cellular uptake of the bCD protein. This conclusion was supported by the (i) 50-fold higher internalization efficiency of bCD−PLL compared to bCD−BF and bCD−AcPLL and (ii) partially blocked bCD−PLL internalization in the presence of polyanionic heparin

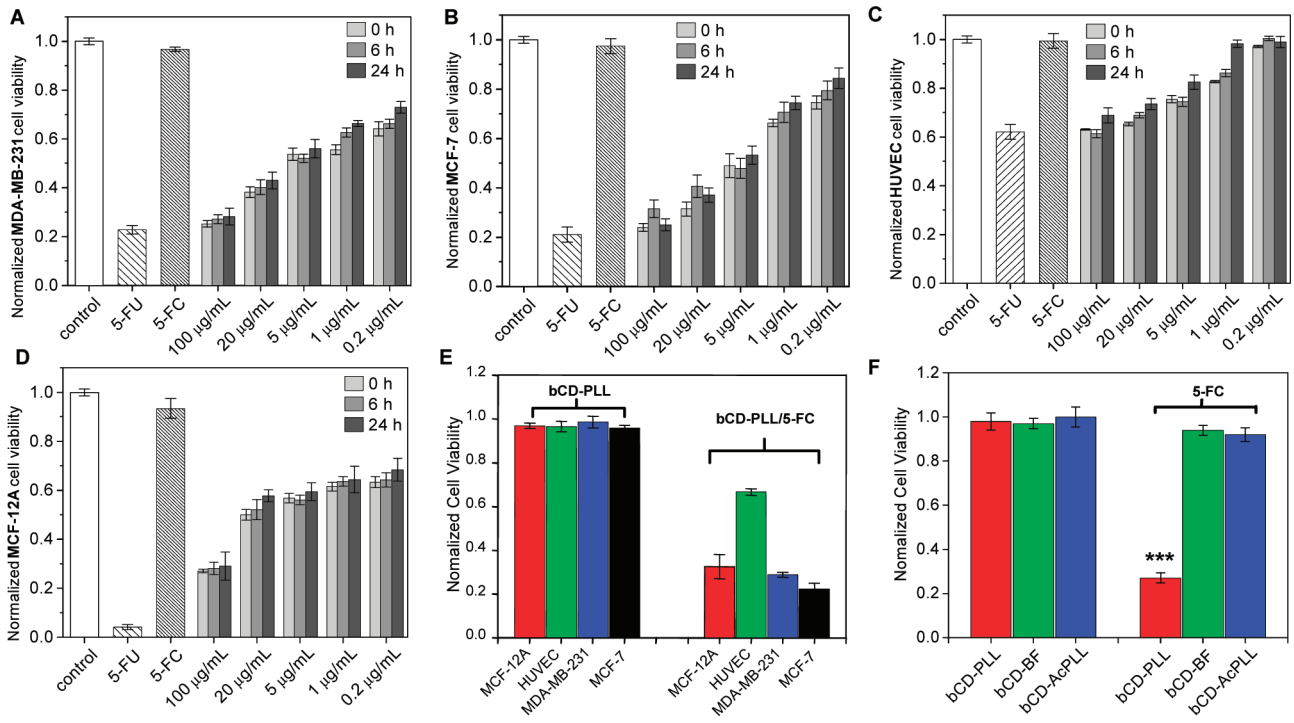

Figure 7. Internalized bCD−PLL but not bCD−BF or bCD−AcPLL maintained high enzymatic stability in cell cultures. MDA-MB-231 (A), MCF-7 (B), MCF-12A (C), and HUVEC (D) cells were treated with bCD−PLL (0.2−100 μg/mL), and 5-FC (1.5 mM, final concentration) was added 0, 6, and 24 h after internalization of this conjugate. In control experiments, cells were untreated or treated with 5-FC (1.5 mM) alone or with 5-FU (1.5 mM) alone. (E) MDA-MB-231, MCF-7, MCF-12A, and HUVEC cells were treated with bCD−PLL (100 μg/mL), and 5-FC (1.5 mM) was added 24 h after the enzyme internalization. In control experiments, cells were treated with bCD−PLL (100 μg/mL) alone without the addition of prodrug. (F) MDA-MB-231 cells were treated with 100 μg/mL bCD−PLL, bCD−BF, or bCD−AcPLL, and 5-FC (1.5 mM) was added 24 h after the enzyme internalization. In control experiments, cells were treated with 100 μg/mL bCD conjugate alone without addition of prodrug. Cell viabilities were measured by the MTT assay. The cell viabilities were presented as mean values ± SD from eight replicated wells: (***) $P < 0.001$, compared with bCD−BF or bCD−AcPLL. All experimental details are described in the Experimental Section.

demonstrating the importance of the electrostatic interaction between PLL and the cell surface. Flow cytometry and confocal microscopic studies further delineated the internalization mechanism of bCD−PLL in live cultured cells. The data clearly indicate that uptake of bCD−PLL, at least for MDA-MB-231 cells, predominately occurs by clathrin-mediated endocytosis. This conclusion is supported by (i) the effective block of bCD−PLL uptake at 4 °C, which suggests that the internalization of bCD−PLL is energy-dependent and involved in an endocytotic mechanism, (ii) the colocalization of bCD−PLL with clathrin-mediated endocytotic marker, transferrin, in live cells, (iii) the substantially decreased cellular uptake of both bCD−PLL and transferrin in the presence of the clathrin-mediated endocytosis inhibitor, chlorpromazine, and (iv) the uncompromised colocalization coefficient between bCD−PLL and transferrin in the presence of inhibitors that impair other endocytotic pathways. Clathrin-mediated endocytosis is documented as a fast cellular uptake pathway.[28] Giacca et al. demonstrated fluorophore-labeled transferrin was internalized into HeLa cells rapidly, with >80% uptake completed within 15 min.[21] However, we observed a much slower cellular uptake of bCD−PLL, and a 50% transduction required more than 8 h. A slow internalization rate of bCD−PLL was also evident with single transferrin-stained vesicles in the cytoplasm of live MDA-MB-231 cells after treatment with a mixture of bCD−PLL and transferrin for 15 min (Figure 6F1). This may be explained in part by the work of Chan et al. where it was demonstrated that the rate of clathrin-mediated endocytosis of transferrin-coated gold nanoparticles decreased in a size dependent manner with the largest particles being internalized at the lowest rates.[29] The molecular weight of bCD−PLL was characterized as 345 kDa with a hydrodynamic diameter of 24.4 nm. Therefore, the relative slow uptake of bCD−PLL was most likely explained by the bulky nature of the bCD protein. Hildt et al. reported that bCD without the transduction domain cannot be internalized into hepatoma cells.[30] However, we indeed observed the cellular uptake of bCD−BF and bCD−AcPLL in MDA-MB-231 cells (Figure 3C). Even though the mechanism of internalization of bCD−BF and bCD−AcPLL remains to be investigated, our study clearly demonstrated that the bound polycationic PLL moiety significantly improved delivery of bCD into the cytoplasm of cultured cells.

We observed that the uptake of bCD−PLL was not restricted to the cell type, although the uptake efficiency was cell line dependent. Flow cytometry studies revealed that the uptake efficiency of bCD−PLL was highest in the highly malignant MDA-MB-231 cell line, compared to the weakly tumorigenic MCF-7 cells and nontumorigenic MCF-12A cells. An overexpression of negatively charge sulfated proteoglycans on the membrane of MDA-MB-231 cells compared with that of MCF-7 and MCF-12A cells has been previously observed.[31] Thus, some of the variations in the bCD−PLL uptake in different cell lines may be caused by differences in population, composition, and size of sulfated proteoglycans as well as phospholipids on the cell membrane. Surprisingly, the uptake of bCD−PLL in HUVEC was higher compared to MCF-7 and MCF-12A cells. This result may be explained by the presence of high affinity membrane-associated glycoproteins such as gp60, which function by stimulating transcellular transport via caveolar-mediated endocytosis in endothelial cells.[32] Within the scope of our studies, the greatly enhanced uptake of bCD−PLL observed in malignant cell lines could prove advantageous as a means to

deliver of high doses of therapeutic agents in a relatively specific manner. Analysis of confocal microscopic images revealed that the average diameters of fluorescent vesicles in human breast cancer MDA-MB-231 and MCF-7 cells were about 7 times larger than that of nonmalignant MCF-12A cells, suggesting that bCD−PLL may be potentially useful to image tumor lesions at very early stages by intravital microscopic imaging.

High enzymatic activity of internalized bCD−PLL was verified by the cytotoxicity induced during incubation of cells with the prodrug. Internalized bCD−PLL exhibited excellent enzymatic stability, and only a slight loss of cytotoxicity was observed when 5-FC was added 24 h after enzyme internalization. bCD−PLL localization, observed at the perinuclear areas of the cytoplasm, will lead to the production of a high concentration of 5-FU and its metabolites that disrupt DNA and RNA synthesis in proximity to the nucleus, where synthesis of DNA and RNA occurs.[33] Endothelial HUVECs were not sensitive to 5-FU, which may be explained by the low 5-FU metabolic rate in nontransformed cells, and this implies a low cytotoxicity of the bCD−PLL/5-FC strategy to vasculature in vivo. Immortalized nontumorigenic MCF-12A breast epithelial cells showed the highest sensitivity to 5-FU. However, only moderate cytotoxicity was observed in MCF-12A cells upon exposure of internalized bCD−PLL to 5-FC, which was likely due to the low cellular uptake of bCD−PLL in MCF-12A cells. Marginal cytotoxicity induced by internalized bCD−BF or bCD−AcPLL compared to bCD−PLL following 5-FC treatment in MDA-MB-231 cells further verified the ability of the polycationic PLL moiety facilitating internalization and maintaining intracellular enzymatic activity.

In summary, our study clearly demonstrates that conjugating PLL to bCD substantially enhances the therapeutic efficacy by accelerating cellular uptake rate while maintaining enzymatic stability in the cytoplasm. This robust enzymatic activity and stability of internalized bCD−PLL in cancer cells provide the extended time required to allow excretion of the enzyme from circulation and normal tissues in vivo to minimize systemic toxicity. The conjugated PLL provides a multivalent modification platform that permits labeling with a high payload of imaging reporters, targeting ligands, and other functional groups without compromising the enzymatic activity of bCD. Further studies characterizing the immunonogenicity of the bCD−PLL conjugate are needed.

Acknowledgment. This work was supported by NIH Grant P50 CA103175 (JHU ICMIC Program) and Grant R21 CA128957. The authors thank Dr. Barry Stoddard of the Fred Hutchinson Cancer Research Center for providing the pET-bCD expression vector. We thank Drs. Michal Neeman, Venu Raman, and Peter Senter for helpful discussions. We thank Drs. Maria Mikhaylova and Noriko Mori for their technical assistance and Dr. Kristine Glunde for guidance with the microscopy. We gratefully acknowledge the support of Dr. J. S. Lewin.

References

(1) Hassett, M. J.; O'Malley, A. J.; Pakes, J. R.; Newhouse, J. P.; Earle, C. C. Frequency and cost of chemotherapy-related serious adverse effects in a population sample of women with breast cancer. *J. Natl. Cancer Inst.* **2006**, *98*, 1108–1117.

(2) Szakacs, G.; Paterson, J. K.; Ludwig, J. A.; Booth-Genthe, C.; Gottesman, M. M. Targeting multidrug resistance in cancer. *Nat. Rev. Drug Discovery* **2006**, *5*, 219–234.

(3) Xu, G.; McLeod, H. L. Strategies for enzyme/prodrug cancer therapy. *Clin. Cancer Res.* **2001**, *7*, 3314–3324.

(4) Ramnaraine, M.; Pan, W.; Goblirsch, M.; Lynch, C.; Lewis, V.; Orchard, P.; Mantyh, P.; Clohisy, D. R. Direct and bystander killing of sarcomas by novel cytosine deaminase fusion gene. *Cancer Res.* **2003**, *63*, 6847–6854.

(5) Ou-Yang, F.; Lan, K. L.; Chen, C. T.; Liu, J. C.; Weng, C. L.; Chou, C. K.; Xie, X.; Hung, J. Y.; Wei, Y.; Hortobagyi, G. N.; Hung, M. C. Endostatin−cytosine deaminase fusion protein suppresses tumor growth by targeting neovascular endothelial cells. *Cancer Res.* **2006**, *66*, 378–384.

(6) Haisma, H. J.; Sernee, M. F.; Hooijberg, E.; Brakenhoff, R. H.; v.d. Meulen-Muileman, I. H.; Pinedo, H. M.; Boven, E. Construction and characterization of a fusion protein of single-chain anti-CD20 antibody and human beta-glucuronidase for antibody-directed enzyme prodrug therapy. *Blood* **1998**, *92*, 184–190.

(7) Kievit, E.; Bershad, E.; Ng, E.; Sethna, P.; Dev, I.; Lawrence, T. S.; Rehemtulla, A. Superiority of yeast over bacterial cytosine deaminase for enzyme/prodrug gene therapy in colon cancer xenografts. *Cancer Res.* **1999**, *59*, 1417–1421.

(8) Egeblad, M.; Werb, Z. New functions for the matrix metalloproteinases in cancer progression. *Nat. Rev. Cancer* **2002**, *2*, 161–174.

(9) Gocheva, V.; Joyce, J. A. Cysteine cathepsins and the cutting edge of cancer invasion. *Cell Cycle* **2007**, *6*, 60–64.

(10) Chauhan, A.; Tikoo, A.; Kapur, A. K.; Singh, M. The taming of the cell penetrating domain of the HIV Tat: myths and realities. *J. Controlled Release* **2007**, *117*, 148–162.

(11) Derossi, D.; Joliot, A. H.; Chassaing, G.; Prochiantz, A. The third helix of the Antennapedia homeodomain translocates through biological membranes. *J. Biol. Chem.* **1994**, *269*, 10444–10450.

(12) Stroh, C.; Held, J.; Samraj, A. K.; Schulze-Osthoff, K. Specific inhibition of transcription factor NF-kappaB through intracellular protein delivery of I kappaBalpha by the Herpes virus protein VP22. *Oncogene* **2003**, *22*, 5367–5373.

(13) Jiang, T.; Olson, E. S.; Nguyen, Q. T.; Roy, M.; Jennings, P. A.; Tsien, R. Y. Tumor imaging by means of proteolytic activation of cell-penetrating peptides. *Proc. Natl. Acad. Sci. U.S.A.* **2004**, *101*, 17867–17872.

(14) Li, C.; Winnard, P. T., Jr.; Takagi, T.; Artemov, D.; Bhujwalla, Z. M. Multimodal image-guided enzyme/prodrug cancer therapy. *J. Am. Chem. Soc.* **2006**, *128*, 15072–15073.

(15) Li, C.; Penet, M. F.; Winnard, P., Jr.; Artemov, D.; Bhujwalla, Z. M. Image-guided enzyme/prodrug cancer therapy. *Clin. Cancer Res.* **2008**, *14*, 515–522.

(16) Rejman, J.; Bragonzi, A.; Conese, M. Role of clathrin- and caveolae-mediated endocytosis in gene transfer mediated by lipo- and polyplexes. *Mol. Ther.* **2005**, *12*, 468–474.

(17) Tyagi, M.; Rusnati, M.; Presta, M.; Giacca, M. Internalization of HIV-1 tat requires cell surface heparan sulfate proteoglycans. *J. Biol. Chem.* **2001**, *276*, 3254–3261.

(18) Brodsky, F. M.; Chen, C. Y.; Knuehl, C.; Towler, M. C.; Wakeham, D. E. Biological basket weaving: formation and function of clathrin-coated vesicles. *Annu. Rev. Cell Dev. Biol.* **2001**, *17*, 517–568.

(19) Seglen, P. O.; Grinde, B.; Solheim, A. E. Inhibition of the lysosomal pathway of protein degradation in isolated rat hepatocytes by ammonia, methylamine, chloroquine and leupeptin. *Eur. J. Biochem.* **1979**, *95*, 215–525.

(20) Wadia, J. S.; Stan, R. V.; Dowdy, S. F. Transducible TAT-HA fusogenic peptide enhances escape of TAT-fusion proteins after lipid raft macropinocytosis. *Nat. Med.* **2004**, *10*, 310–315.

(21) Fittipaldi, A.; Ferrari, A.; Zoppe, M.; Arcangeli, C.; Pellegrini, V.; Beltram, F.; Giacca, M. Cell membrane lipid rafts mediate caveolar endocytosis of HIV-1 Tat fusion proteins. *J. Biol. Chem.* **2003**, *278*, 34141–34149.

(22) West, M. A.; Bretscher, M. S.; Watts, C. Distinct endocytotic pathways in epidermal growth factor-stimulated human carcinoma A431 cells. *J. Cell Biol.* **1989**, *109*, 2731–2739.

(23) Johannes, L.; Lamaze, C. Clathrin-dependent or not: is it still the question. *Traffic* **2002**, *3*, 443–451.

(24) Nori, A.; Kopecek, J. Intracellular targeting of polymer-bound drugs for cancer chemotherapy. *Adv. Drug Delivery Rev.* **2005**, *57*, 609–636.

(25) Trinh, Q. T.; Austin, E. A.; Murray, D. M.; Knick, V. C.; Huber, B. E. Enzyme/prodrug gene therapy: comparison of cytosine deaminase/5-fluorocytosine versus thymidine kinase/ganciclovir enzyme/prodrug systems in a human colorectal carcinoma cell line. *Cancer Res.* **1995**, *55*, 4808–4812.

(26) Uzgiris, E. The role of molecular conformation on tumor uptake of polymeric contrast agents. *Invest. Radiol.* **2004**, *39*, 131–137.

(27) Aime, S.; Gianolio, E.; Terreno, E.; Giovenzana, G. B.; Pagliarin, R.; Sisti, M.; Palmisano, G.; Botta, M.; Lowe, M. P.; Parker, D. Ternary Gd(III)L-HSA adducts: evidence for the replacement of inner-sphere water molecules by coordinating groups of the protein. Implications for the design of contrast agents for MRI. *J. Biol. Inorg. Chem.* **2000**, *5*, 488–497.

(28) Conner, S. D.; Schmid, S. L. Regulated portals of entry into the cell. *Nature* **2003**, *422*, 37–44.

(29) Chithrani, B. D.; Chan, W. C. Elucidating the mechanism of cellular uptake and removal of protein-coated gold nanoparticles of different sizes and shapes. *Nano Lett.* **2007**, *7*, 1542–1550.

(30) Hillemann, A.; Brandenburg, B.; Schmidt, U.; Roos, M.; Smirnow, I.; Lemken, M. L.; Lauer, U. M.; Hildt, E. Protein transduction with bacterial cytosine deaminase fused to the TLM intercellular transport motif induces profound chemosensitivity to 5-fluorocytosine in human hepatoma cells. *J. Hepatol.* **2005**, *43*, 442–450.

(31) Gowda, D. C.; Bhavanandan, V. P.; Davidson, E. A. Isolation and characterization of proteoglycans secreted by normal and malignant human mammary epithelial cells. *J. Biol. Chem.* **1986**, *261*, 4926–4934.

(32) Shajahan, A. N.; Timblin, B. K.; Sandoval, R.; Tiruppathi, C.; Malik, A. B.; Minshall, R. D. Role of Src-induced dynamin-2 phosphorylation in caveolae-mediated endocytosis in endothelial cells. *J. Biol. Chem.* **2004**, *279*, 20392–20400.

(33) Longley, D. B.; Harkin, D. P.; Johnston, P. G. 5-fluorouracil: mechanisms of action and clinical strategies. *Nat. Rev. Cancer* **2003**, *3*, 330–338.

JM800288H